Stream gauge calibration of a cave stream using water temperature variability as a tracer

Lüthi, Martin P

Abstract: Calibration of stream gauging stations involves water velocity measurements at various water levels to obtain discharge and to determine the rating curve. This process is laborious, often logistically challenging, or even impossible for streams that are only accessible at low flow. Here, we present an alternative method to obtain mean stream velocity by matching temperature variation patterns measured at two positions in the stream. Such water temperature variations are caused by snow melt or rainfall events and serve as natural tracers. The method is successfully applied to a karst cave stream that is only accessible at lowest flow. The installed high-precision data loggers provide sufficient data to obtain a relationship between water depth and mean velocity. The approximate rating curve, based on reach mean channel width, agrees well with results from dye tracer experiments. This cave stream shows the typical features of a steep step-pool stream such as a power law relation between mean velocity and discharge.

DOI: https://doi.org/10.1029/2018wr023762

Water Resources Research

RESEARCH ARTICLE
10.1029/2018WR023762

Stream Gauge Calibration of a Cave Stream Using Water Temperature Variability as a Tracer

M. P. Lüthi[1]

[1]Department of Geography, University of Zurich, Zurich, Switzerland

Key Points:
- Water temperature variability is used as natural tracer for stream velocity
- This facilitates stream gauge calibration of mostly inaccessible cave streams
- Our step-pool stream shows a power-law velocity-discharge relation

Correspondence to:
M. P. Lüthi,
martin.luethi@geo.uzh.ch

Citation:
Lüthi, M. P. (2019). Stream gauge calibration of a cave stream using water temperature variability as a tracer. *Water Resources Research*, *55*. https://doi.org/10.1029/2018WR023762

Received 24 JUL 2018
Accepted 6 JUN 2019
Accepted article online 11 JUN 2019

Abstract Calibration of stream gauging stations involves water velocity measurements at various water levels to obtain discharge and to determine the rating curve. This process is laborious, often logistically challenging, or even impossible for streams that are only accessible at low flow. Here, we present an alternative method to obtain mean stream velocity by matching temperature variation patterns measured at two positions in the stream. Such water temperature variations are caused by snow melt or rainfall events and serve as natural tracers. The method is successfully applied to a karst cave stream that is only accessible at lowest flow. The installed high-precision data loggers provide sufficient data to obtain a relationship between water depth and mean velocity. The approximate rating curve, based on reach mean channel width, agrees well with results from dye tracer experiments. This cave stream shows the typical features of a steep step-pool stream such as a power law relation between mean velocity and discharge.

1. Introduction

Calibrating stream gauges requires records of water level and discharge at various flow conditions. Discharge is conventionally determined by measurements of cross-sectional profiles and by in situ measurements of mean stream velocity during repeated field campaigns (Comiti et al., 2007; Turnipseed & Sauer, 2010; WMO, 2010). Obtaining river rating curves therefore is a laborious, often logistically challenging process, and measurement uncertainties are often difficult to quantify (Hamilton & Moore, 2012). For streams located in extreme topography direct calibration of stream gauges might even be impossible. Many such rivers, such as steep mountain streams, rivers in narrow gorges, or underground karst streams are often only safely accessible at low flow.

Dilution gauging by means of dye tracers is an alternative approach that is particularly well suited for steep streams with complex channel topography or streams that cannot be gauged accurately using the velocity-area method (Schneider et al., 2015). In these cases, analysis of tracer breakthrough curves yields the mean stream velocity or directly the discharge (Moore, 2005; Richardson et al., 2017; Zimmermann, 2010). Again, performing a comprehensive series of such tracer tests at different water levels requires substantial field efforts.

Water temperature is a natural tracer, which evolution can be described with the heat advection-dispersion equation (e.g., Covington et al., 2011). Heat energy is, of course, not a conservative tracer and is affected by heat exchange processes with the environment. On shorter distances, infiltration in river beds has been tracked by water temperature measurements (e.g., Dogwiler et al., 2007; Hatch et al., 2006). This method tracks mainly the seepage flow vertical to the main stream direction, although slow hyporheic flow can be tracked as well (e.g., Zlotnik & Tartakovsky, 2018).

In confined settings that are isolated from direct radiation and the atmosphere, water temperature has been used to derive information on horizontal flow velocities such as groundwater flow (e.g., Anderson, 2005; Saar, 2011; Somogyvári & Bayer, 2017; Wigley & Brown, 1971). In karst stream networks, heat exchange with the environment is usually dominated by conduction in the surrounding rock (Covington et al., 2011; Luhmann et al., 2015) such that advected heat is a suitable tracer for water flow (e.g., Benderitter et al., 1993; Long & Gilcrease, 2009; Luhmann et al., 2011).

Here we present a method to calibrate stream gauges in a cave stream with minimal field effort by simply logging water pressure and temperature at very high precision and rate. Since lateral heat exchange with the

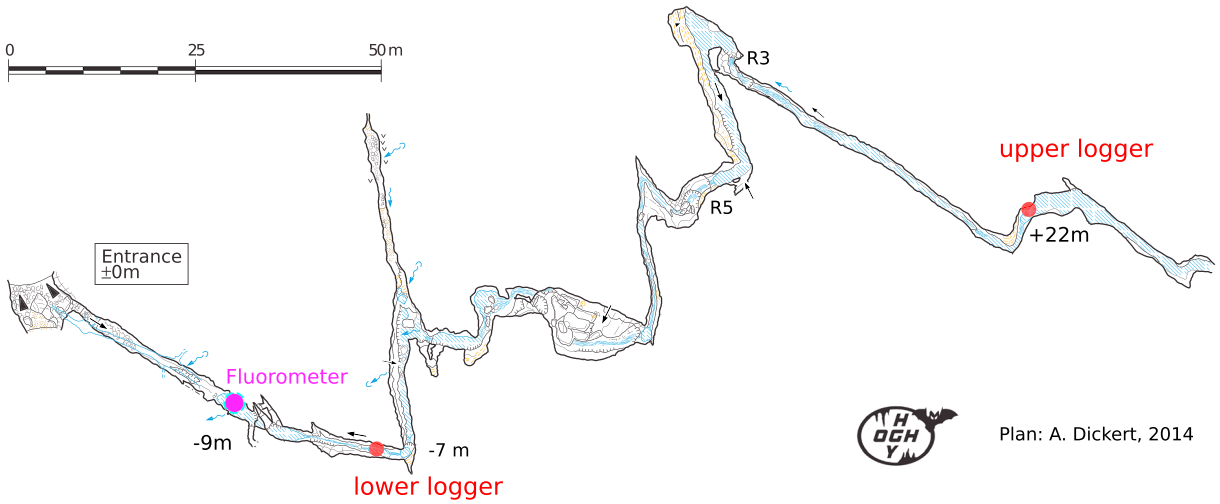

Figure 1. Relevant part of the map of the Kreuzloch cave system. The positions of the data loggers are indicated by red dots, and the fluorometer with a purple dot. R3 and R5 are small waterfalls of 3 and 5 m height. Numbers indicate the elevation with respect to the cave entrance.

cave walls and longitudinal dispersion are both small, the method consists of matching similar patterns of temperature variations at several positions along the stream. From the travel times of temperature patterns, average water flow speeds can be determined, from which an approximate water pressure-discharge relation (rating curve) is obtained under the assumption of constant mean stream width. This relation is confirmed by results from several experiments with fluorescent dye dilution.

2. Methods

2.1. Field Site

An active karst cave system, which is relatively easy to access, was chosen as experimental site. The cave of Kreuzloch, Unteriberg, Switzerland, which features three perennial streams and which has been accurately mapped, is ideal for this experiment, as the stream is not exposed to solar radiation. The main cave stream is accessible over 800 m, with major confluences at about 260 and 600 m from the cave entrance. The cave stream collects the water from two perennial sinks (Riedloch/Hinterofen and Chalberalpeli), which were used for dye-tracing experiments. Underground distances amount to estimated 2.5 km from the cave entrance (most of the passages are inaccessible).

Figure 1 shows the relevant part of the cave map with the positions where loggers for temperature and pressure were deployed. Data from two loggers, which were placed in a section without confluence, were used for this study. For the fluorescent dye tracer tests a submersible fluorometer was temporarily installed close to the cave entrance.

2.2. Instrumentation

Several RBRduet-T.D oceanographic data loggers equipped with high-precision pressure and temperature sensors were deployed at different positions along the accessible cave stream. The loggers were protected within steel pipes, which were mounted on the rock walls with heavy-duty M10 rock anchors (Figure 2). The data acquisition interval was set to 2 s, which allowed continuous measurements for more than a year.

Resolution and absolute accuracy for pressure were 5 and ±250 Pa, corresponding to 0.05 and ±2.5 mm water level, respectively. Temperature was recorded with 0.05 mK resolution and ±2 mK absolute accuracy. The time constants for the pressure and temperature sensors are <10 ms and ~1 s and were only marginally altered by the protecting steel pipes.

The loggers register absolute pressure, which had to be corrected for air pressure variations. For three months (April to June), a MSR-165 data logger at the cave entrance registered air pressure, temperature, and humidity. The air pressure agreed well with variations registered by the meteorological station Einsiedeln at some 20 km distance. The corrections to the water pressure were made with these continuous records in an hourly interval, corrected for the elevation difference, and linearly interpolated.

Figure 2. Logger installation in the cave stream. The data logger is protected within a steel pipe, which is fixed to the cave wall with a M10 rock bolt. The temperature and pressure sensors at the bottom of the pipe are in direct contact with the flowing water. Width of the passage is about 1.3 m.

2.3. Instrument Synchronization

Precise synchronization of the data loggers is mandatory for an accurate estimation of travel times. From our experience, the RBR logger clocks show shifts of less than 2 s after a year of deployment. All sensors were programmed with computers synchronized through the network time protocol, from which synchronization errors of less than a second should be expected.

To unambiguously synchronize all loggers, they were submerged at once during 60 s into water, and the times of dumping and recovery were exactly determined from a handheld GPS receiver. These submersion events are recorded in the pressure data and were used to validate the synchronization and to correct for inaccuracies in the sensor clocks. The accuracy of this synchronization is of the order of the measurement interval (2 s in our case).

2.4. Matching Algorithm

The determination of average water flow speed hinges on the accurate detection of water temperature change patterns. For a short section (minutes to hour) of the temperature record at the upstream sensor with an interesting pattern, we searched for the same pattern in the temperature record of the downstream sensor. If such a section has been found, an optimization yields the two parameters travel time Δt and temperature change ΔT, as illustrated in Figure 3. While the first parameter always fulfills $\Delta t > 0$, the second parameter can be both positive and negative, as heat is exchanged with air and the surrounding rock (Covington et al., 2011).

To achieve the task of automatically obtaining many travel time measurements, the above matching procedure was repeatedly applied. The data loggers provide values of pressure p_i and temperature T_i at times t_i with a measurement interval of 2 s in our experiment. Travel times were determined at regularly spaced times t_j (we used an interval of 10 min). A set of data array indices corresponding to a search window Δt_w (we choose 60 min) was determined by

$$\mathcal{J}_j = \left[i \quad | \quad t_i >= t_j - \Delta t_w ; t_i <= t_j + \Delta t_w \right] . \tag{1}$$

The temperatures of the downstream sensor were linearly interpolated to yield a function $\mathcal{T}(t)$ that can be evaluated at any time t. For suitable time windows an optimizer (Nelder-Mead or BOBYQA from the NLOPT

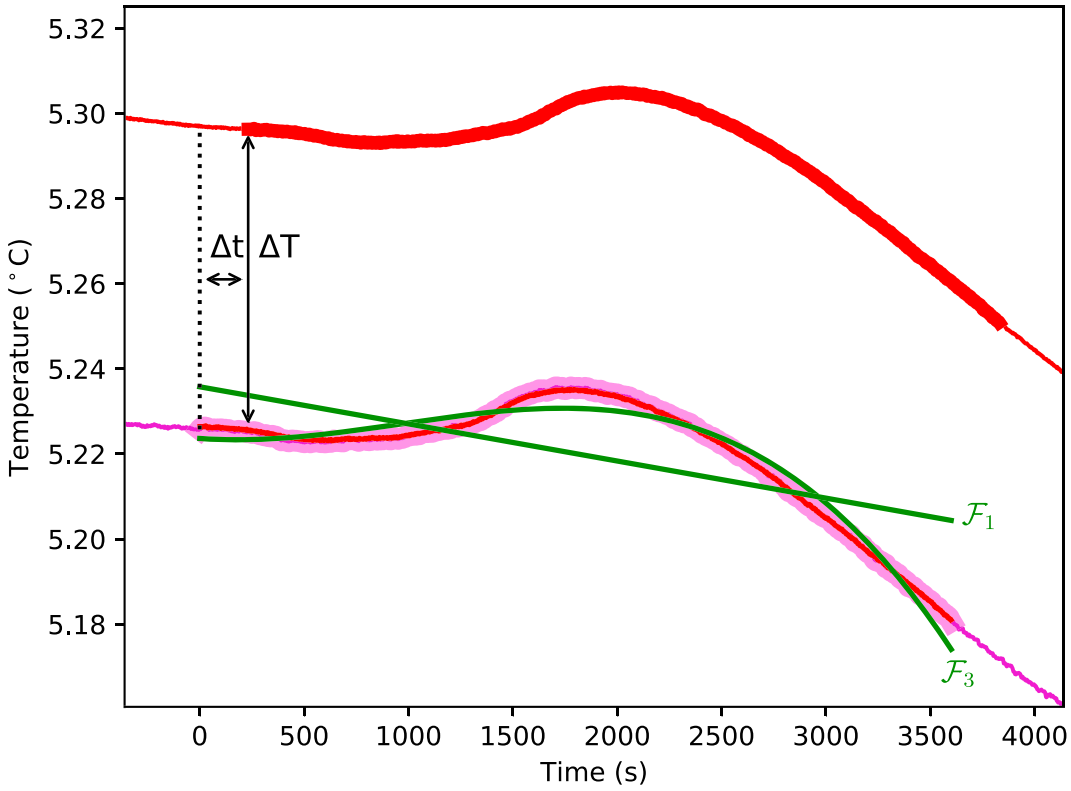

Figure 3. Illustration of the matching procedure. Thin lines are the temperature variations of the upstream (purple) and downstream (red) sensors. Wide lines indicate the time windows used for the matching procedure, which were prescribed for the purple curve and determined for the red curve. Through an optimization procedure the parameters Δt and ΔT were obtained, which shift the red curve onto the purple. Green lines indicate the polynomials of first ($\mathcal{F}_1$) and third ($\mathcal{F}_3$) degree, which are used to quantify the nonlinearity of the signal that is needed for a successful determination of travel time.

optimization library; Johnson, 2012) was used to determine the best fit of the two temperature curves. The objective function (cost function) to minimize was defined by

$$\mathcal{G}(\Delta t, \Delta T) = \sum_{i \in J_j} \left(\mathcal{T}(t_i + \Delta t) - T_i + \Delta T\right)^2, \tag{2}$$

from which the travel time Δt and the temperature change ΔT were determined. The optimizer was started with the expected time difference that was roughly estimated from a mean flow velocity of 0.5 m s^{-1} and the distance. The expected temperature difference ΔT_{exp} was calculated as the warming by complete dissipation of potential energy

$$\Delta T_{exp} = \frac{g}{C}\Delta z \simeq 2.345\,\mathrm{mK\,m^{-1}} \cdot \Delta z = 0.068\,\mathrm{K}, \tag{3}$$

where $g = 9.81$ m s^{-2} is the gravity, $C = 4182\,\mathrm{J kg^{-1}\ K^{-1}}$ is the specific heat capacity of water, and Δz is the elevation difference of the sensors (29 m in our case).

2.5. Matching Interval Determination

An algorithm was devised to automatically decide whether the temperature variability in a chosen time interval contains enough signal for the matching procedure and thus is suitable for the detection of travel time. Since a constant temperature change rate cannot be used to uniquely identify a matching pattern, the deviation from linearity has to be determined. For this purpose, two polynomials were fitted through the temperature data for each time interval, a linear $\mathcal{F}_1$ and a cubic $\mathcal{F}_3$. The mean and maximum differences of these temperature fits provide a robust estimate whether the signal within the interval is sufficiently

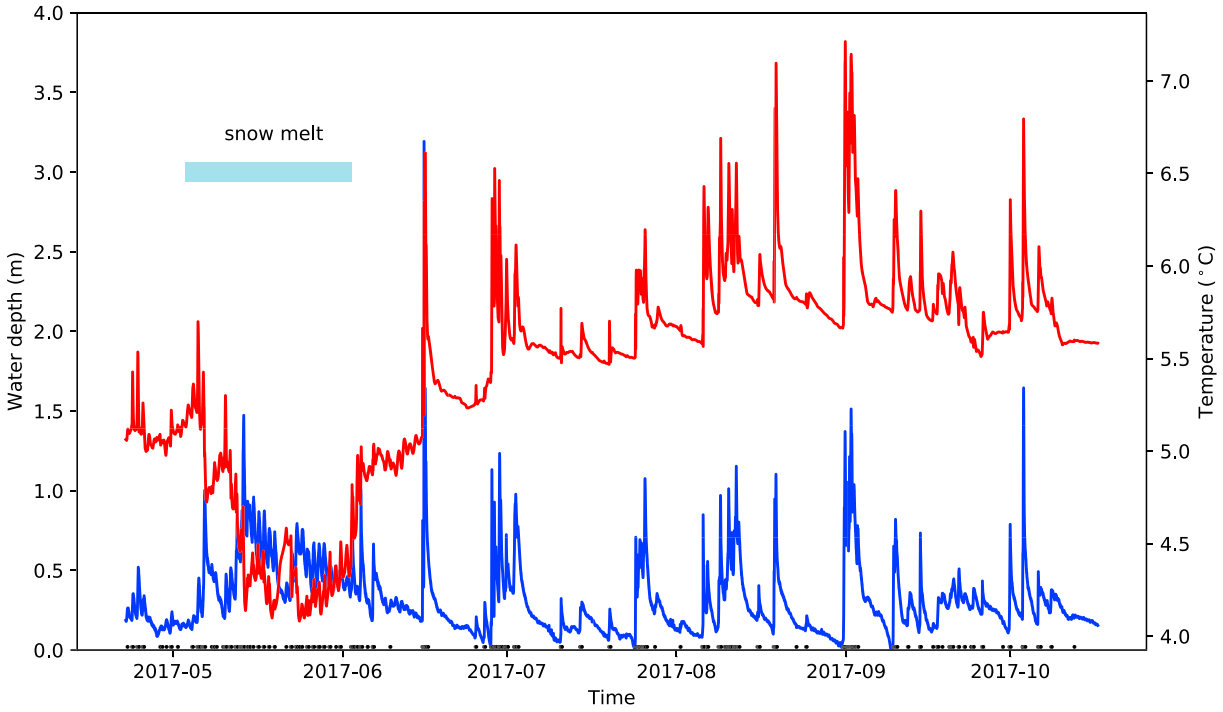

Figure 4. The time series of water depth (blue) and water temperature (red) at the upper logger for mid-April to mid-October 2017. The snow melt period is indicated by a blue bar. Black dots at the bottom indicate time windows that were used to determine the water flow speed.

nonlinear and therefore contains enough variability for the matching procedure. A matching for travel time was only performed if both of the following conditions held

$$\begin{aligned} \max\left(\left|\mathcal{F}_3 - \mathcal{F}_1\right|\right) &>= a_{\max}, \\ \text{mean}\left(\left|\mathcal{F}_3 - \mathcal{F}_1\right|\right) &>= a_{\text{mean}}, \end{aligned} \tag{4}$$

where the thresholds $a_{\max} = 0.003\,\text{K}$ and $a_{\text{mean}} = 0.002\,\text{K}$ were determined by trial and error for the temperature resolution of our sensors.

2.6. Dye Tracer Experiments

The concentration of the fluorescent dye Uranine in the cave stream was continuously measured with an autonomous logging fluorometer installed 20 m into the cave from the entrance (Figure 1). The fluorometer of type Turner C3 was programmed to log data in a 20 s interval for two longer measurement campaigns (50 hr duration; "Chalberalpeli" and "Riedloch" in Figures 6 and 7) and in a 1-s interval for the tests in the cave stream at lowest discharge ("Kreuzloch").

From the measured dye tracer concentration $c(t)$ the discharge Q was calculated using the expression (e.g., Kilpatrick & Cobb, 1985)

$$Q = m_{\text{inj}} \left(\int_{t_{\text{inj}}}^{t_{\text{rem}}} c(t)\,dt \right)^{-1}, \tag{5}$$

where m_{inj} is the mass of the injected tracer and t_{inj} and t_{rem} are the times of injection and of removal of the fluorometer, respectively.

3. Results

Water temperature and pressure were recorded during the snow melt and summer seasons between April and October 2017 in an interval of 2 s at two loggers in the cave stream. Figure 4 shows the data from the upper logger. Clearly visible is the diurnal snow melt between mid-May to early June, which lowers the water temperature considerably. During this period, water height and temperature are mostly anticorrelated.

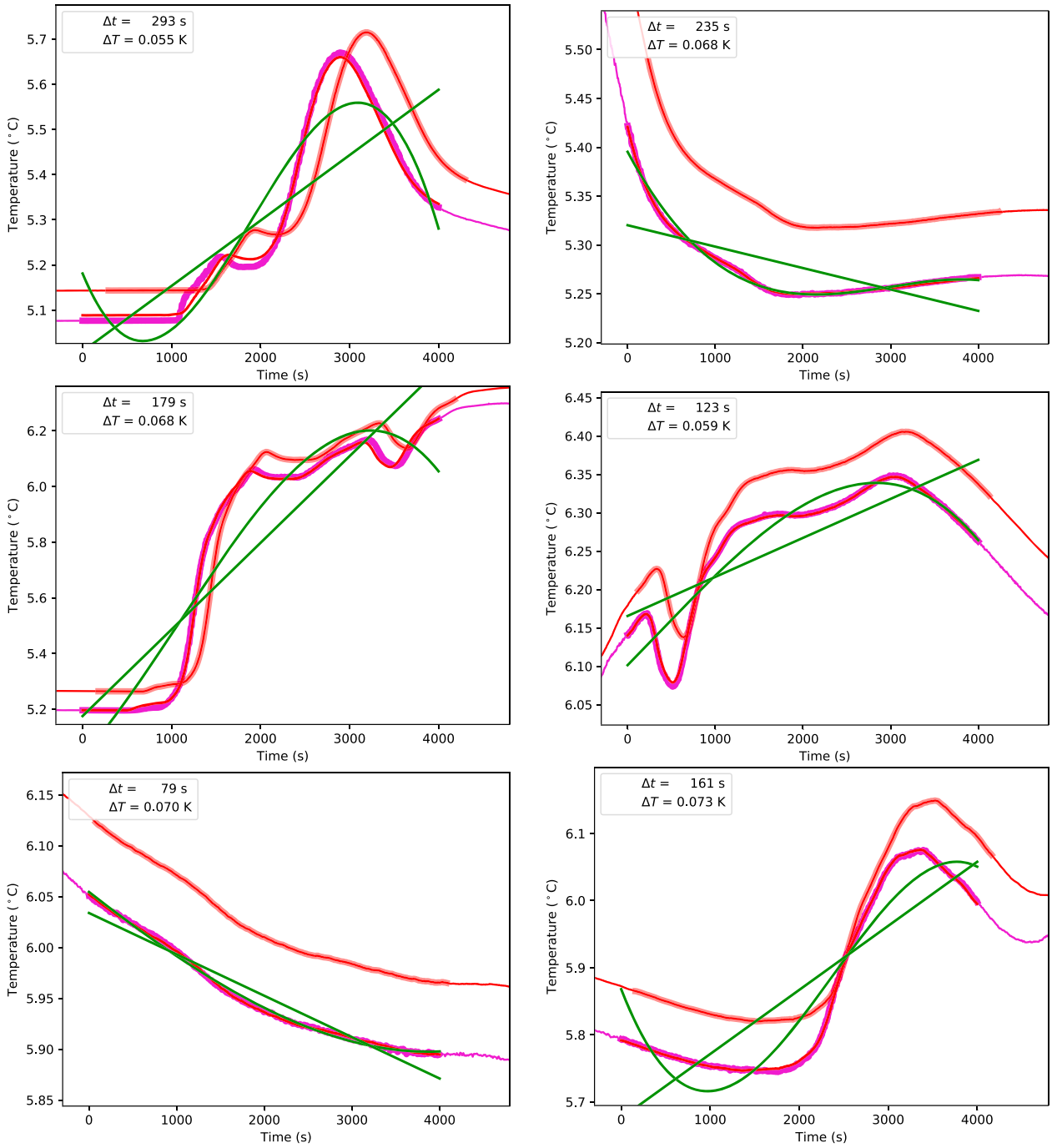

Figure 5. Several examples of temperature variations at the upper (purple) and lower (red) logger. Wide line sections indicate the matching window of 4,000 s in both curves, the red solid line on top of the purple wide line is the matched section. Values of Δt and ΔT in the boxes indicate the results of the matching procedure. Green lines indicate the polynomials of first ($\mathcal{F}_1$) and third ($\mathcal{F}_3$) degree, which are used to quantify the nonlinearity of the signal.

In summer, high water pressures are due to precipitation and violent thunderstorms, which coincide with rapid and considerable warming of the cave stream.

Water temperature variations due to snow melt and thunderstorms were used as a natural tracer to determine the average flow speed between the two loggers in 242.4 m distance and with an elevation drop of 29 m (12 % average slope). Suitable patterns of temperature variability of the upstream logger were identified with the method described in section 2.5. Matching these patterns with the record of the downstream logger, using the algorithm of section 2.4, yielded the travel times Δt of the water between the two positions. Figure 5

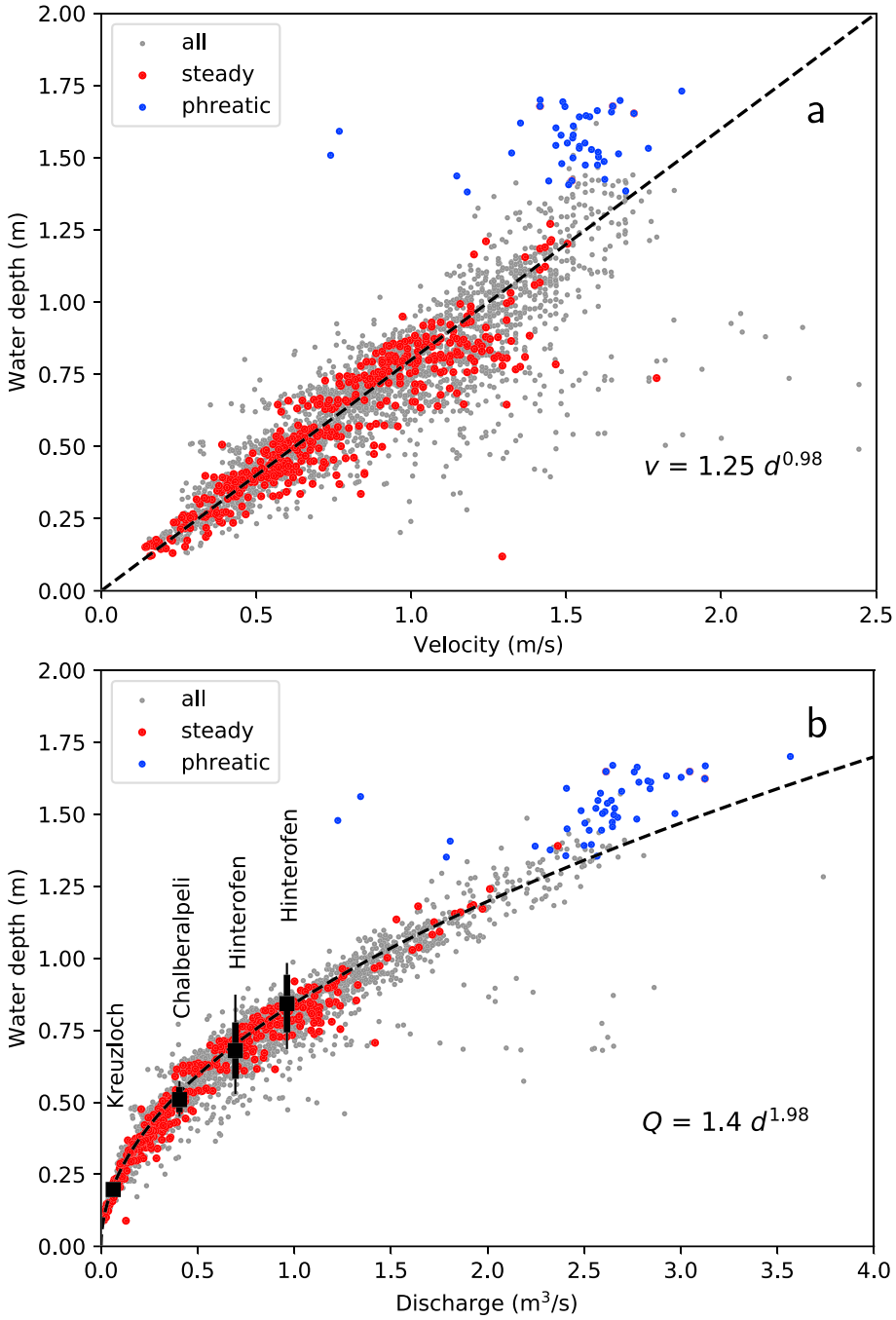

Figure 6. Relationship between water depth and mean flow velocity (a) and discharge (b). Black dots show all ~2,000 measurements, red dots the ~700 measurements with steady conditions, and blue dots the measurements under phreatic conditions. The dashed line is a least squares fit of a power law through the red points. Black squares and vertical lines in (b) indicate discharge determined with fluorescent dye tracer experiments, while vertical lines indicate the range of water levels in unsteady flow during these experiments.

illustrates a few typical patterns. For roughly 2,000 time intervals during the 6 months of data recording, a robust estimate of travel time could be determined. These intervals are indicated by black dots in Figure 4.

Figure 6 shows the ~2,000 average stream flow velocities v plotted against water depth d at the upper logger. Since water depths at both loggers during steady conditions agree to within 0.05 m (0.02 m standard deviation), only data from the upper logger are shown. The wide spread of the values and the isolated points far from the curve are likely due to the unsteady flow of the stream during storm surges. Plotting only the

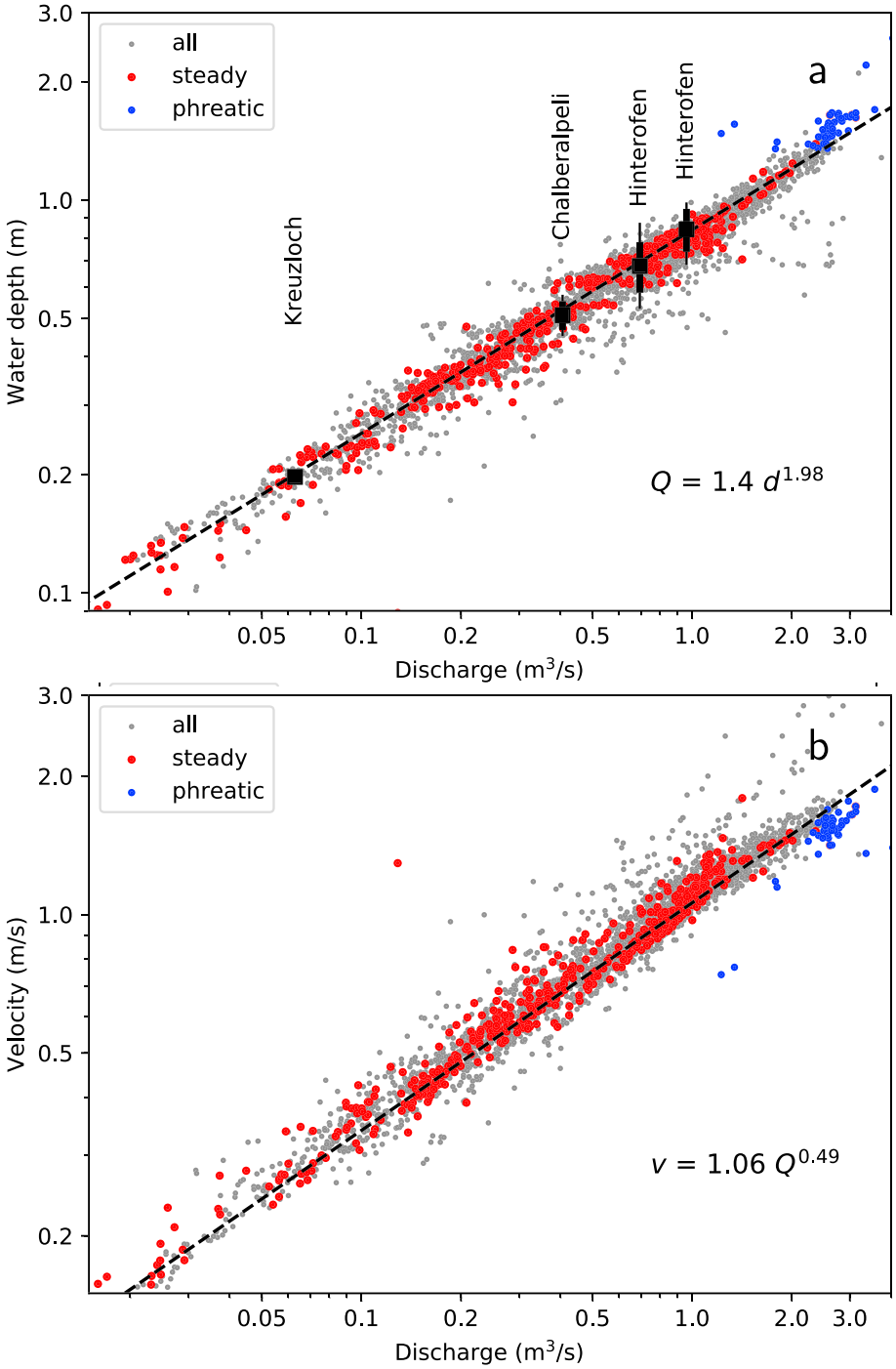

Figure 7. (a) The power law relation between discharge and water depth. (b) The power law relation between discharge and mean flow velocity. The meaning of symbols is the same as in Figure 6.

Table 1
Characteristic Quantities of the Fluorescent Dye Tracer Experiments Conducted in Summer 2018

Injection site	Date	L	m_{inj}	d	Q	D_L
		(m)	(g)	(m)	($m^3 s^{-1}$)	(m^2 s)
Hinterofen	2018-05-05	~2,500	272	0.84	0.962	0.089
Hinterofen	2018-08-25	~2,500	61	0.68	0.695	0.087
Chalberalpeli	2018-06-01	~2,500	180	0.51	0.406	0.033
Kreuzloch	2018-09-29	260	3	0.20	0.063	0.002

Note. The approximate flow distance L, the injected mass m_{inj} of Uranine, the water depth d at the data logger, and the discharge Q calculated with equation (5) are given. The longitudinal dispersion D_L results from analysis of the tracer breakthrough curves.

~700 points with near-steady conditions reduces the spread of the data points considerably (red dots in the figure). Steady conditions were assumed when the water depth variation was less than ± 0.03 m hr^{-1}.

The data points under steady conditions (red dots in Figure 6a) cluster around a nearly linear fitting line ($r^2 = 0.92$; $\sigma = 0.09$ m s^{-1}) given by

$$v \simeq 1.25 d^{0.98}. \tag{6}$$

At water depths exceeding ~2 m several sections of the bedrock channel become completely water filled, and the flow conditions in the cave stream become partially phreatic. These conditions seem to limit mean stream flow velocity at around 1.5 m s^{-1} (marked with blue dots in Figure 6).

To derive the discharge, the determined reach mean flow velocity was multiplied by the average channel width and the flow depth at the pressure sensor. Since the channel walls are nearly vertical, we used the average width $w = 1.12$ m throughout the probed section to obtain

$$Q = vwd \simeq 1.4 d^{1.98}, \tag{7}$$

$d^{1.98}$. This relation was validated through dye tracer tests. The rationale for using reach average and local quantities is discussed in section 4.2.

Four tracer experiments with the fluorescent dye Uranine were conducted in summer 2018, and characteristic numbers are given in Table 1. The comparison of the discharge determined by dye dilution with the rating curve is shown in Figures 6b and 7a. The agreement of this independent validation of the rating curve (equation (7)) is reaffirming. The considerable uncertainty in water depth indicated with error bars is due to unsteady flow conditions during the tracer tests at high flow and over long distance ("Chalberalpeli" and "Hinterofen").

4. Discussion

4.1. Prerequisites

The method of obtaining mean stream velocity from water temperature variability hinges on a few conditions that need to be fulfilled to obtain meaningful results. The main prerequisite is a well-mixed stream already upstream of the loggers such that water temperature can be assumed homogeneous within the stream cross-section. For a steep step-pool stream with many small water falls, like our cave stream, this condition is certainly satisfied (e.g., Comiti et al., 2007; Schneider et al., 2015), as a mixing length of less than 25 wetted widths has been determined with salt dilution tests (Richardson et al., 2017). Furthermore, the probed stream section should be free of major inflows and leakages.

Heat exchange with the environment should be small and homogeneous along the stream. Our stream is protected from shortwave radiation and interacts only with the air and rocks in the cave by turbulent heat exchange and longwave radiation. Deviations of water temperature from the annual average are within 1.5 ° C, which drives only small lateral heat fluxes. Consequently, stream temperature patterns are very similar at both sites, as illustrated in Figure 5.

Some tens to hundreds of detectable temperature change patterns at different water levels are necessary to obtain a stable rating curve. In our karst cave environment the stream temperature variations are due to

diurnal snow melt events and rain storms. We used 6 months of data, although only using May and June with peak snow melt and first summer thunder storms yielded very similar results.

4.2. Velocity-Discharge Relation

Water flow speed of steep streams with step-pool geometry is not well described by the conventionally used Darcy-Weisbach relation but is better reproduced by power law relations between mean stream velocity, discharge, and water depth (Comiti et al., 2007; Reid et al., 2010; Rickenmann, 1991; Schneider et al., 2015; Zimmermann, 2010). Exactly this type of relation has been found in equations (6) and (7). These equations can be rewritten for comparison with other publications in terms of a velocity-discharge curve

$$v = k Q^m , \tag{8}$$

with $k = 1.06$ and $m = 0.49$ for our data. The exponent m obtained here differs somewhat from the values 0.55 or 0.6 found by others (Schneider et al., 2015; Zimmermann, 2010) but agrees with the mean values 0.49 and 0.51 obtained by Comiti et al. (2007) and Reid et al. (2010) for steep mountain streams.

The calculation of discharge in equation (7) mixes reach mean velocity and channel width with the locally measured flow depth. To obtain a proper discharge estimate, the mean wetted cross-sectional area along the stream section would be needed. Both width and flow depth have been related to discharge by power laws (e.g., Comiti et al., 2007; Reid et al., 2010). In our deeply incised stream the width is nearly constant with depth but varies substantially along the stream. The local flow depth, however, is unknown. It is likely related to local flow speed by a power law similar to equation (6), albeit with spatially varying parameters (Reid et al., 2010). Without additional assumptions on the power law parameters, additional measurements at high flow, or calibration with independent discharge measurement, the parameters k and m in equation (8) remain poorly constrained.

The reason why our simple and approximate discharge calculation (equation (7)) agrees with independent discharge measurements is likely due to the repeating stream morphology. The major part of the investigated reach consists of similar steps and pools, such that our measurements are representative for many of them. Both pressure sensors, showing nearly identical water depth variability, were installed within the laminar outflow of pools of similar width. At this position the flow speed is close to the average, with higher speeds over the steps and lower speeds in the pools, as exemplified by measurements in an experimental flume (Lee, 1998, chapter 10).

Flume experiments and field measurements have shown that the increasing submergence of obstacles at high discharge leads to reduced relative roughness and friction. The influence of channel roughness is reduced, and the along-stream variability decreases (e.g., Church & Zimmermann, 2007; Lee, 1998; Lee & Ferguson, 2002). It therefore seems reasonable to assume that the difference between mean flow velocity and the velocity at the pressure sensor decreases at high flow, which again justifies the use of equation (7).

4.3. Error Sources

The established relation between water depth and discharge in equation (6) was obtained from hundreds of travel time determinations at steady flow conditions. Nevertheless, the point cloud in Figure 6 exhibits a relatively wide spread of velocities with a standard deviation of 0.09 m s^{-1} even during the phases of constant water depth. Possible causes of this wide spreadare discussed in the following.

Instrumentation errors are very unlikely to cause the observed spread of values. Both loggers were placed at the side walls in shallow pools with high currents, and temperature sensor tips were flush with the ends of the protecting steel pipes. The temperature sensors have an adjustment time scale of 1 s, such that observed maximum delays of the temperature readings were less than two readings, that is, 4 s, and the pressure sensors react much faster.

The stream bed consists throughout of solid limestone bedrock with many steps, potholes, and little waterfalls of 0.5 to 3 m height. The water flow is fully turbulent along most of the 242 m of cave passage such that the stream water is continually well mixed. Boundary layer effects are therefore reduced to a minimum, and determined velocities are expected to be very close to the average bulk velocity of the water that would be obtained with an artificial tracer.

The observed outliers and the wide spread of data values cannot be explained by shortcomings of the measurement procedures. Consequently, poor matching of temperature variability is another possible cause.

Doubling the thresholds a_{mean} or a_{max}, thus selecting more pronounced temperature variability patterns indeed reduces the number of outliers but also seriously reduces the number of matches (by a factor 10), while leaving the fitting curves the same.

Water storage during stationary flow conditions is minimal, as there are no sizable pools in the stream course. This is also reflected in the average flow speeds exceeding 0.1 m s^{-1} even at lowest water levels.

The derivation of the equations assumes a constant stream width at different water depths, a condition which is approximately fulfilled at the logger installation sites. In contrast, along the stream the channel width varies considerably between 0.7 and 2 m, with one cave chamber exceeding 5 m (Figure 1). The average width of the channel is about 1.2 m, and therefore similar to the value assumed to calculate discharge in equation (7). It is difficult to assess how the width variations affect the measured mean flow velocity, but given that the power law (8) between velocity and discharge - which is independent of geometry - describes most steep streams indicates that width variability in step-pool streams is of minor importance.

A further possible cause is heat exchange with the environment. The rock walls that are warmed or cooled during high flow exchange heat with the water (Covington et al., 2011; Luhmann et al., 2015). To influence the velocity determination procedure, such temperature changes would have to be simultaneous over a large section of the stream, and extending far upstream of the upper logger.

Using equation 21 from Luhmann et al. (2015) yields delays of the temperature signal of 3 to 60 s for a temperature signal of 1,000 s duration at high or low flow. This delay changes determined velocity by 1% to 3%.

An estimate of lateral heat exchange between stream and surrounding rock can be obtained from the variability of the optimization parameter ΔT. For the whole measurement period the temperature differences between upstream and downstream loggers were within the interval 0.025 to 0.08 K. The mean value of 0.068 K corresponds to the temperature difference expected from complete dissipation of potential energy (equation (3)). An order-of-magnitude estimate of lateral heat flux is thus easily obtained. For high values of temperature difference ($\Delta T_{\max} = 0.04$ K) and discharge ($Q = 3\,m^3s^{-1}$), the heat transferred to the environment is $P = QC\Delta T_{\max} = 3 \cdot 4{,}182 \cdot 0.04$ W ~ 500 W, or 2 W per meter along the stream, where the heat capacity of water $C = 4{,}182$ J/K/kg, or properly J K^{-1} kg^{-1} has been used. Lateral heat exchange is therefore very small and does not influence the results of this study.

Dispersion of the temperature signal potentially affects the precision of the travel time determination. From dye tracer tests listed in Table 1 and earlier work (Bucher, 2015), we infer a longitudinal dispersivity of $D_L = 10^{-3}$ to 10^{-1} m^2 s or m^2s for longer sections L of the cave stream by analysis of fluorescent dye breakthrough curves, yielding Péclet numbers of $\mathrm{Pe} = LV/D_L = 2 \cdot 10^3$ to $5 \cdot 10^5$. Such high values for Pe indicate strongly advection dominated flow where dispersion is effectively switched off. Figure 5 illustrates that the shape of temperature change patterns is conserved and that dispersion is negligible.

Stream stage readings were performed with pressure sensors in the flowing water. These sensors register absolute pressure, which was corrected with data from a distant meteorological station (section 2.2). Air pressure within the cave system follows outside air pressure, but the dynamics of variable air flow might affect the pressure registered within the cave. In addition, the filling and emptying of cave passages during high flow could drive air flow and seriously affect air pressure readings. Since the magnitude of air pressure variations is a significant fraction of the pressure change due to varying water levels, inaccurate air pressure correction is therefore the most likely explanation for the wide spreadd of values in Figure 6. This source of error could potentially be corrected by installation of a pressure logger in air, or by using differential pressure sensors. Obviously, the problem remains during phreatic flow conditions.

4.4. General Applicability of the Method

The proposed method for effortless calibration of stream gauges was developed for data from a karst cave environment without radiative forcing and minimal heat fluxes to the environment (Covington et al., 2011; Luhmann et al., 2015). A similar setting is expected in sewer systems where radiation is of no concern but pipe flow might not be as well mixed as in step-pool cave streams.

It is likely that the method could also be applied in more general settings, notably to calibrate stream gauges in hardly accessible sections of streams with low lateral heat exchange, such as narrow gorges in mountain streams, or streams under a dense canopy. If sunny periods are excluded from the records, the environmen-

tal conditions are likely stable enough to allow for an application of the temperature variability matching procedure. Temperature variability is much more pronounced in surface streams, such that lower accuracy loggers should be able to resolve the stream temperature signal from rain storms and snow melt.

5. Conclusions

A novel method to determine mean stream flow velocity from water temperature variability alone was derived and successfully applied to a cave stream. Together with knowledge on stream geometry, approximate relationships between discharge and stream stage (rating curves) can be derived without any field effort. The laborious procedure of measuring mean water flow speed with physical devices or tracer dilution tests is therefore avoided.

The proposed method uses natural water temperature variability of a well-mixed stream as tracer and requires no other field efforts than installing two high-precision temperature and pressure loggers at a distance of tens to hundreds of meters. The method can be used in extreme environments with little lateral heat exchange where the streams are only safely accessible at lowest discharge, such as narrow gorges, sewer systems, and caves.

For the example site in a cave stream we determined rating curves from hundreds of temperature change patterns that were used to determine mean flow velocity. Application of the method to other settings should be straight forward as long as some crucial prerequisites are fulfilled. Most important are a turbulent, well-mixed current, and the exclusion from data analysis of periods with high lateral heat exchange such as through direct solar radiation. Investigations on the suitability of the method for wider use are currently underway.

Acknowledgments
Funding for instrumentation and part of the work was through research project SNF 200021_156098 by the Swiss National Science Foundation and the Geographical Institute of the University of Zurich. Valuable comments by C. Luce, C. Hatch, D. Irvine, and B. Kurylyk helped improve the presentation. This work was supported by cavers of "Höhlengruppe Ybrig" (HGY) and "Ostschweizerische Gesellschaft für Höhlenforschung" (OGH) through equipping and mapping the cave stream, their help with instrumentation, and the tracer tests, namely, Domenika Bucher, Andreas Dickert, Edwin Fuchs, Richard Graf, Beat Hediger, Christoph Kälin, Markus Kälin, Robert Kälin, and Remo Reichmuth. Additional help in the field was provided by Roland Litschi, Thomas Lüthi, Rémy Mercenier, and Nico Mölg. The support of the Hydrology Group of the University of Zurich, namely, Jan Seibert, Ilja van Meerveld, and Benjamin Fischer, is highly appreciated. The data logger readings are published at Zenodo.org under https://doi.org/10.5281/zenodo.1299718.

References

Anderson, M. P. (2005). Heat as a ground water tracer. *Ground Water*, *43*(6), 951–968. https://doi.org/10.1111/j.1745-6584.2005.00052.x

Benderitter, Y., Roy, B., & Tabbagh, A. (1993). Flow characterization through heat transfer evidence in a carbonate fractured medium: First approach. *Water Resources Research*, *29*(11), 3741–3747. https://doi.org/10.1029/93WR01685

Bucher, D. (2015). Karsthydrologie im Ybrig (SZ) (Master thesis), University of Zurich, Switzerland. pp. 108.

Church, M., & Zimmermann, A. (2007). Form and stability of step-pool channels: Research progress. *Water Resources Research*, *43*, W03415. https://doi.org/10.1029/2006WR005037

Comiti, F., Mao, L., Wilcox, A., Wohl, E. E., & Lenzi, M. A. (2007). Field-derived relationships for flow velocity and resistance in high-gradient streams. *Journal of Hydrology*, *340*, 48–62. https://doi.org/10.1016/j.hydrol.2007.03.021

Covington, M. D., Luhmann, A. J., Gabrovšek, F., Saar, M. O., & Wicks, C. M. (2011). Mechanisms of heat exchange between water and rock in karst conduits. *Water Resources Research*, *47*, W10514. https://doi.org/10.1029/2011WR010683

Dogwiler, T., Wicks, C., & Jenzen, E. (2007). An assessment of the applicability of the heat pulse method toward the determination of infiltration rates in karst losing-stream reaches. *Journal of Cave and Karst Studies*, *69*(2), 237–242.

Hamilton, A., & Moore, R. (2012). Quantifying uncertainty in streamflow records. *Canadian Water Resources Journal*, *37*(1), 3–21. https://doi.org/10.4296/cwrj3701865

Hatch, C. E., Fisher, A. T., Revenaugh, J. S., Constantz, J., & Ruehl, C. (2006). Quantifying surface water-groundwater interactions using time series analysis of streambed thermal records: Method development. *Water Resources Research*, *42*, W10410. https://doi.org/10.1029/2005WR004787

Johnson, S. G. (2012). The NLopt nonlinear-optimization package, http://ab-initio.mit.edu/nlopt

Kilpatrick, F. A., & Cobb, E. D. (1985). Techniques of water-resources investigations (*Tech. Rep. TWI 03-A16*). Reston: U.S. Geological Survey.

Lee, A. (1998). The hydraulics of steep streams (Ph.D. thesis), Department of Geography, Sheffield University. 266 pp.

Lee, A. J., & Ferguson, R. I. (2002). Velocity and f low resistance in step-pool streams. *Geomorphology*, *46*, 59–71.

Long, A. J., & Gilcrease, P. C. (2009). A one-dimensional heat-transport model for conduit flow in karst aquifers. *Journal of Hydrology*, *378*, 230–239. https://doi.org/10.1016/j.jhydrol.2009.09.024

Luhmann, A., Covington, M., Myre, J., Perne, M., Jones, S., Alexander, E. Jr., & Saar, M. (2015). Thermal damping and retardation in karst conduits. *Hydrology and Earth System Sciences*, *19*, 137–157. https://doi.org/10.5194/hess-19-137-2015

Luhmann, A. J., Covington, M. D., Peters, A. J., Alexander, S. C., Anger, C. T., Green, J. A., et al. (2011). Classification of thermal patterns at karst springs and cave streams. *Ground Water*, *49*(3), 324–335.

Moore, R. D. (2005). Introduction to salt dilution gauging for streamflow measurement part 3: Slug injection using salt in solution. *Streamline Watershed Management Bulletin*, *8*(2), 1–6.

Reid, D. E., Hickin, E. J., & Babakaiff, S. C. (2010). Low-flow hydraulic geometry of small, steep mountain streams in southwest British Columbia. *Geomorphology*, *122*, 39–55. https://doi.org/10.1016/j.geomorph.2010.05.012

Richardson, M., Moore, R. D., & Zimmermann, A. (2017). Variability of tracer breakthrough curves in mountain streams: Implications for streamflow measurement by slug injection. *Canadian Water Resources Journal*, *42*(1), 21–37. https://doi.org/10.1080/07011784.2016.1212676

Rickenmann, D. (1991). Hyperconcentrated flow and sediment transport at steep slopes. *Journal of Hydraulic Engineering*, *117*(11), 1419–1439.

Saar, M. (2011). Review: Geothermal heat as a tracer of large-scale groundwater flow and as a means to determine permeability fields. *Hydrogeology Journal*, *19*, 31–52. https://doi.org/10.1007/s10040-010-0657-2

Schneider, J., Rickenmann, D., Turowski, J., & Kirchner, J. W. (2015). Self-adjustment of stream bed roughness and flow velocity in a steep mountain channel. *Water Resources Research*, *51*, 7838–7859. https://doi.org/10.1002/2015WR016934

Somogyvári, M., & Bayer, P. (2017). Field validation of thermal tracer tomography for reconstruction of aquifer heterogeneity. *Water Resources Research*, *53*, 5070–5084. https://doi.org/10.1002/2017WR020543

Turnipseed, D., & Sauer, V. (2010). Discharge measurements at gaging stations, *U.S. Geological Survey Techniques and Methods book 3, chap. A8*. Reston, Virginia: U.S. Geological Survey.

WMO (2010). Manual on stream gauging (*Tech. Rep. 1044*). Geneva, Switzerland: World Meteorological Organization.

Wigley, T., & Brown, M. C. (1971). Geophysical applications of heat and mass transfer in turbulent pipe flow. *Boundary-Layer Meteorology*, *1*, 300–320.

Zimmermann, A. (2010). Flow resistance in steep streams: An experimental study. *Water Resources Research*, *46*, W09536. https://doi.org/10.1029/2009WR007913

Zlotnik, V., & Tartakovsky, D. (2018). Interpretation of heat-pulse tracer tests for characterization of three- dimensional velocity fields in hyporheic zone. *Water Resources Research*, *54*, 4028–4039. https://doi.org/10.1029/2017WR022476